

Scattering of Deuterons in Helium

T. LAURITSEN* AND T. HUUS, *Institute for Theoretical Physics, Copenhagen, Denmark*

AND

S. G. NILSSON, *University of Lund, Lund, Sweden*

(Received September 8, 1953)

The scattering of deuterons in helium gas has been investigated at three angles in the energy range 1000 to 1200 kev. A pronounced resonance appears at $E_d=1069$ kev, of width 35 kev (lab), which corresponds to the 2.187-Mev level of Li^6 . It is established that the level in question has $J=3$, even parity, and a reduced width of the order of the single-particle limit. The best fit to the observations is obtained with a channel radius of 4.0×10^{-13} cm, taking into account the effect of the ground state, $J=1^+$, which is assumed to have the same reduced width. A brief search, carried out at only one angle, revealed no further levels below $E_d=2.0$ Mev.

I. INTRODUCTION

THE scattering of alpha particles by deuterons was investigated in 1935 by Pollard and Margenau,¹ who used natural alpha-particle sources, bombarding thin targets of deuterium-containing compounds and observing the forward-projected deuterons. The alpha-particle energy was varied by means of a gas cell with adjustable pressure. Above an energy of 2.0 Mev, they found strong deviations from Coulomb scattering and in the neighborhood of 2.6 Mev, a pronounced anomaly, nearly 1 Mev broad, which they attributed to a resonance. There was also some indication of a maximum near 5 Mev. Assuming the resonance energy to be $E_\alpha=2.6$ Mev, these measurements would indicate a level of Li^6 at 2.3 Mev above the ground state. Later observations by Mohr and Pringle² indicated a rise in cross section in the neighborhood of 2-Mev alpha-particle energy but did not confirm the resonance. Subsequently, very careful measurements have been made of the scattering of deuterons in helium gas as a

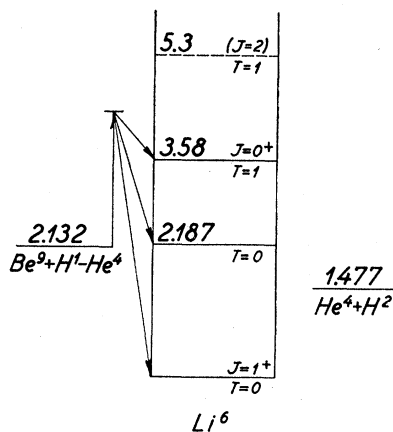


FIG. 1. Energy levels of Li^6 .

function of angle at a number of energies.^{3,4} These measurements straddled the energy at which the resonance might have been expected ($E_d \approx \frac{1}{2} E_\alpha = 1.3$ Mev) and gave no indication of its existence. In the meantime, the Li^6 level in question has been well established in several other reactions, among these in connection with an alpha-particle group⁵ from $\text{Be}^9(p,\alpha)\text{Li}^6$ (Fig. 1). In this measurement, carried out with a precision electrostatic analyzer, the level could be located at 2.187 ± 0.008 Mev; the width was reported to be less than 8 kev. From this information and the known masses involved, it would appear that the resonance in the scattering process should lie at $E_d = 1.065 \pm 0.040$ Mev, or $E_\alpha = 2.13$ Mev.

No little interest attaches to this, the first excited level of Li^6 , since the theory makes a rather definite prediction as to its character.⁶ For a system with only two particles in the p shell, one expects levels of $J=1^+$ and 3^+ , with isotopic spin $T=0$, to lie fairly low, in either $L-S$ or $j-j$ coupling. In pure $j-j$ coupling, the $(p_{3/2}, p_{3/2})$ configuration leads to states of $J=3^+$, 0^+ , 1^+ , and 2^+ , with $T=0, 1, 0$, and 1 , in order of increasing energy, while in $L-S$ coupling, the low states are 3S_1 , $^3D_3, 2, 1$ with $T=0$, and 1S_0 , $T=1$. Even a slight admixture of $j-j$ coupling in the latter case will separate the components of the D -triplet and tend to lower the $J=3$ member. The ground state of Li^6 has $J=1$, $T=0$, and the magnitude of the magnetic moment suggests that the character 3S_1 predominates for this state. The 3.58-Mev state⁷ appears to have $J=0$ or $T=1$ or both, and from the mass of He^6 it is reasonably safe to conclude that this is the first $T=1$ level. A level at about 5.3 Mev, also with $T=1$ and, possibly $J=2^+$ is suggested by analogy with the first excited state of He^6 . It would seem, then, that the 2.187-Mev level has $T=0$, and probably $J=3^+$. Because of the circumstance

³ N. P. Heydenburg and R. B. Roberts, Phys. Rev. **56**, 1092 (1939).

⁴ Blair, Freier, Lampi, and Sleator, Phys. Rev. **75**, 1678 (1949).

⁵ Browne, Williamson, Craig, and Donahue, Phys. Rev. **83**, 179 (1951).

⁶ D. R. Inglis, Phys. Rev. **87**, 915 (1952); Revs. Modern Phys. **25**, 390 (1953).

⁷ R. B. Day and R. L. Walker, Phys. Rev. **85**, 582 (1952).

* Fulbright Lecturer (1952-1953), on leave from California Institute of Technology, Pasadena, California.

¹ E. Pollard and H. Margenau, Phys. Rev. **47**, 833 (1935).

² C. B. O. Mohr and G. B. Pringle, Proc. Roy. Soc. (London) **A160**, 190 (1937).

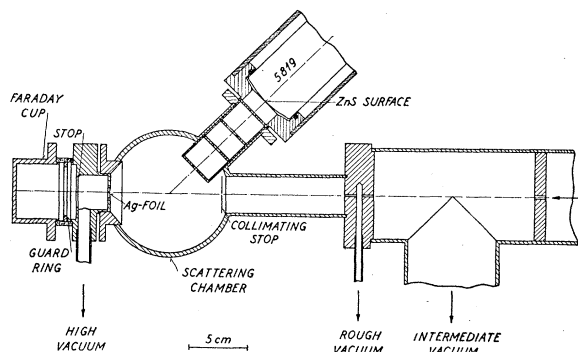


FIG. 2. Schematic diagram of the scattering chamber and differential pumping system.

that the level is unbound with respect to $\text{He}^4 + \text{D}^2$, the scattering of deuterons in helium should provide a particularly favorable opportunity for a direct determination of the angular momentum and parity, and it was with this objective that the present experiments were undertaken. It was also hoped that a systematic search in the immediately higher excitation region might shed some light on the location of the two other D states, which would be expected if $L-S$ coupling obtains for this nucleus.

II. EXPERIMENTAL PROCEDURE

Since the resonance was expected to be only a few kev wide, a gas target at relatively low pressure, separated from the accelerator by a differential pumping system, was used. The experimental arrangement is shown in Fig. 2. Deuterons from the 2-Mev electrostatic accelerator of this Institute⁸ were analyzed by a 7.5° magnetic deflection. The beam then passed through a 3-mm hole into the intermediate chamber, which was held at $\sim 10^{-4}$ mm Hg by a 3-in. diffusion pump. A 1.0-mm diameter channel 10 mm long separated this chamber from the rough-pump vacuum of $\sim 5 \times 10^{-2}$ mm Hg, which was further separated from the scattering chamber, at 1- to 10-mm pressure, by an 0.8-mm

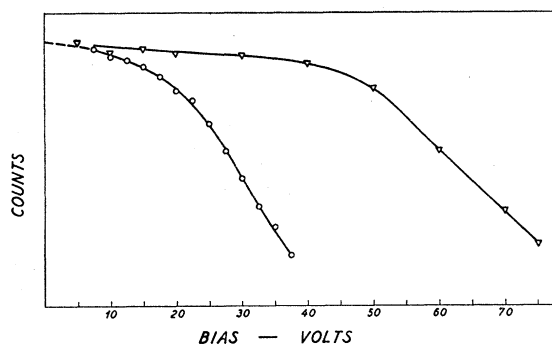


FIG. 3. Typical integral bias curves, obtained with monoenergetic protons. The upper curve refers to 260-kev protons; the lower, to 140-kev protons.

⁸ Brostrom, Huus, and Tangen, Phys. Rev. **71**, 661 (1947).

diameter channel, 10 mm long. After passing through the scattering chamber, the beam entered the Faraday cage through a 7-mm hole which was covered by an 0.9-mg/cm^2 Ag foil. The Faraday cage was maintained at high vacuum by a direct connection to the accelerating tube.

An auxiliary stop, 1.2 mm in diameter, located 5 cm above the center of the scattering chamber was used in the work at low bombarding energy to reduce the effect of compound scattering in the gas and to insure that all the current actually passed through the 7-mm aperture of the Faraday cage. Rough computations, verified by direct observation of the beam, indicated that this requirement was amply met under the conditions of the present experiments. The limiting stops and guard ring of the Faraday cage were designed to accept particles diverging from the foil by angles up to 20° and should therefore have accepted more than 99 percent of protons or deuterons of 500 kev.

The scattering volume and angle were defined by two rectangular apertures $l=10$ mm high (perpendicular

TABLE I. Comparison of check determinations with previously published values.

	$d\sigma/d\Omega$ (barn/sterad)		
		Standard	Present experiment
$\text{O}^{16}(p,p)\text{O}^{16}$, $E_p=0.6$ Mev, $\theta_{\text{cm}}=90^\circ$	0.97 ^a	1.00	± 0.06
$\text{He}^4(p,p)\text{He}^4$, $E_p=0.96$ Mev, $\theta_{\text{cm}}=77^\circ$	0.112 ^b	0.104	± 0.005
$\text{He}^4(d,d)\text{He}^4$, $E_d=1.96$ Mev, $\theta_{\text{cm}}=156^\circ$	0.109 ^c	0.11	± 0.01

^a Rutherford cross section plus 5 percent, as estimated from curves of F. Eppling, kindly communicated by Professor H. T. Richards. See also W. Wenzel and W. Whaling, Phys. Rev. **87**, 499 (1952).

^b Interpolated from data of Freier, Lampi, Sleator, and Williams, Phys. Rev. **75**, 1345 (1949).

^c Interpolated from data of reference 4.

to the plane of the incident beam and the axis of the collector slits) and of width $2b=0.27$ and $2a=0.52$ cm, respectively. They were separated by a distance $h=7.5$ cm and the rear-most was $R=10.3$ cm from the intersection of the axis with the beam. It can readily be shown that the product (solid angle \times target thickness) is given by $\int \Omega dx = 4alb / (Rh \sin\theta)$, where θ is the angle of scattering, and that the effective target thickness is $2bR / (h \sin\theta)$. In the present case, for $\theta=135^\circ$, $\int \Omega dx$ was 2.99×10^{-3} steradian cm (laboratory coordinates), and the target thickness was 0.54 cm, corresponding to an energy loss at 1.0 Mev of 0.07 kev per mm of He pressure. The angular resolution was 4.2° (lab) full width at half maximum. Three ports were available, making angles of 135.8° , 90.0° , and 63.8° with the direction of the beam.

Detection of the scattered particles was accomplished by means of a thin layer of activated zinc sulfide on the end of a 5819 photomultiplier tube. Direct light from the deuteron beam was excluded by a layer of Au foil 0.2 mg/cm^2 thick laid directly on the ZnS surface. Residual light effects due to incomplete opacity of the

gold foil could be measured by interposing a quartz window in the path of the scattered particles.

The matter of obtaining easily interpretable bias curves occasioned some difficulty. At the back angle, where high amplification was necessary, the curve rose rapidly for low bias settings, presumably because of small pulses from electron trapping effects. It was found that the largest ratio of "true" to "spurious" pulse size, i.e., the most satisfactory plateau, was obtained with a not quite opaque layer of ZnS, corresponding to an efficiency of about 80 percent. At the forward angle, recoil alpha particles interfered to some extent. Rather than cut the alpha particles out with absorbers, which would have increased the straggling of the deuterons, we preferred to use a set of "normal curves," for matching to the curves obtained in the scattering experiment. The normal curves, of which two examples are shown in Fig. 3, were obtained with both protons and deuterons, scattered from a copper target

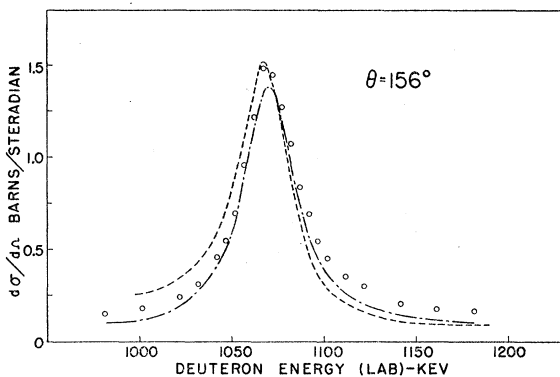


FIG. 4. Differential scattering cross section for deuterons in helium, $\theta_{cm} = 156^\circ$. Experimental points are indicated by the open circles. The dot-dashed curve is calculated for one resonance, $J = 3^+$, $l = 2$ with channel radius $R = 4.02 \times 10^{-13}$ cm, whereas the dashed curve is calculated for $R = 6.55 \times 10^{-13}$ cm.

and monochromatized with a magnetic spectrometer. The absolute efficiency was measured at a proton energy of 1.0 Mev by comparison with a proportional counter, and the relative efficiency was checked at various energies by measuring the Rutherford scattering in copper in the same instrument. The efficiency at 1.0 Mev was found to be 0.78 ± 0.03 ; down to the lowest energy investigated, ~ 140 keV, it was constant within the experimental error of about 10 percent.

As a check both on the efficiency determination and on other quantities entering into the final measurement, the scattering cross sections for protons in oxygen and for protons and deuterons in helium were measured at points for which values have been given in the literature. The results, exhibited in Table I, indicate a mean deviation of the present measurements from the assumed standards of less than 5 percent.

The helium used was certified by the supplier to be 99.9 percent pure; it was further purified by prolonged

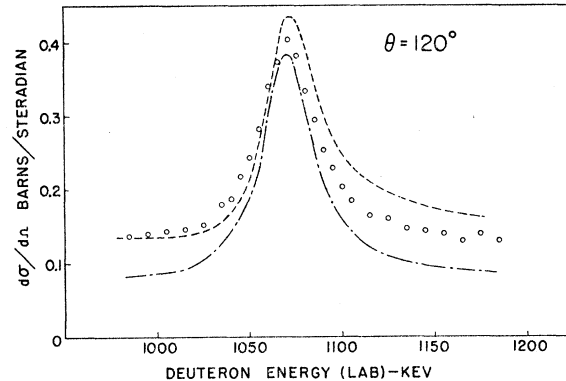


FIG. 5. Differential cross section at $\theta_{cm} = 120^\circ$. Open circles are experimental points. The dot-dashed curve is calculated for one resonance, $J = 3^+$, $l = 2$ with $R = 4.02 \times 10^{-13}$ cm; the dashed curve is calculated for $R = 6.55 \times 10^{-13}$ cm.

storage in contact with liquid-air-cooled charcoal. A similar trap directly connected to the scattering chamber prevented contamination from incidental gas sources. The oxygen was also certified to be 99.9 percent pure: it was freed of any possible condensibles by contact with a liquid-air trap.

III. RESULTS

The observed differential scattering cross section as a function of bombarding energy for three angles is exhibited by the open circles in Figs. 4, 5, and 6. It is immediately apparent that a strong resonance exists, as expected, in the neighborhood of 1070 keV bombarding energy. At the two back angles, θ (center of mass) $= 156^\circ$ and 120° , the maximum cross section occurs at 1069 ± 2 keV and the width at half-maximum is about 35 keV. For the 90° observations (Fig. 6) the resonance is characterized by a minimum, occurring at 1075 keV. A survey run at the 156° angle, taken with 20-keV intervals, revealed no further structure at higher energies. Above the resonance, the cross section falls off to 0.11 barn/steradian at about 1300 keV and remains within 10 percent of this value to 2.0 Mev.

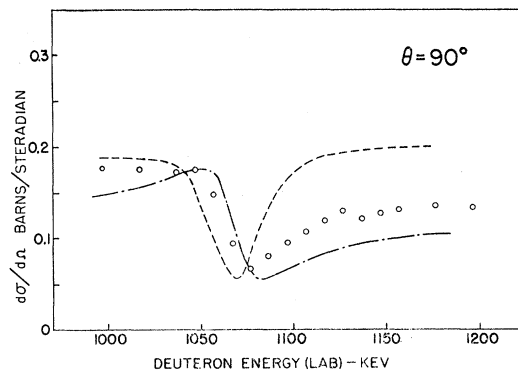


FIG. 6. Differential cross section at $\theta_{cm} = 90^\circ$. The dot-dashed curve is calculated for one resonance, $J = 3^+$, $l = 2$, with $R = 4.02 \times 10^{-13}$ cm; the dashed curve is the same, with $R = 6.55 \times 10^{-13}$ cm.

TABLE II. Absolute cross-section determinations, $\text{He}^4(d,d)\text{He}^4$.

E_d (lab) keV	$d\sigma/d\Omega$ (barns/steradian)		
	1000	1069	1200
$\theta_{\text{cm}} = 156^\circ$	0.15 ± 0.03	1.49 ± 0.08	0.16 ± 0.03
$\theta_{\text{cm}} = 120^\circ$	0.14 ± 0.01	0.40 ± 0.03	0.14 ± 0.01
$\theta_{\text{cm}} = 90^\circ$	0.18 ± 0.02	0.062 ± 0.006	0.14 ± 0.02

A number of separate runs was made at the peak and in the wings of the resonance to establish the absolute cross sections. These observations were made under varying conditions of gas pressure and geometry in order to eliminate as far as possible any systematic errors. The weighted mean values so obtained are given in Table II together with the probable errors, estimated from the reproducibility of individual points and from the uncertainty in the absolute efficiency of the detector at 1 Mev. The values at maximum have been used to normalize the cross-section scale for the experimental points in the figures.

IV. DISCUSSION

The scattering formula for particles of spin 1 impinging on a spin zero nucleus can be written, in the one-level approximation:⁹

$d\sigma/d\Omega$

$$\begin{aligned}
&= \frac{2}{3}\lambda^2 |A_e + \sum_l \left\{ \frac{1}{2}(l+2) \exp(i\delta_{l,l+1} + i\psi_l) \sin\delta_{l,l+1} \right. \\
&\quad + \frac{1}{2}(2l+1) \exp(i\delta_{l,l} + i\psi_l) \sin\delta_{l,l} \\
&\quad + \frac{1}{2}(l-1) \exp(i\delta_{l,l-1} + i\psi_l) \sin\delta_{l,l-1} \left. \right\} P_l(\cos\theta)|^2 \\
&\quad + \frac{2}{3}\lambda^2 |A_e + \sum_l \left\{ (l+1) \exp(i\delta_{l,l+1} + i\psi_l) \sin\delta_{l,l+1} \right. \\
&\quad + l \exp(i\delta_{l,l-1} + i\psi_l) \sin\delta_{l,l-1} \left. \right\} P_l(\cos\theta)|^2 \\
&\quad + \frac{2}{3}\lambda^2 \left| \sum_l \frac{1}{\sqrt{2l(l+1)}} \left\{ l(l+2) \exp(i\delta_{l,l+1} + i\psi_l) \sin\delta_{l,l+1} \right. \right. \\
&\quad - (2l+1) \exp(i\delta_{l,l} + i\psi_l) \sin\delta_{l,l} \\
&\quad \left. \left. - (l-1) \exp(i\delta_{l,l-1} + i\psi_l) \sin\delta_{l,l-1} \right\} \sin\theta \frac{dP_l(\cos\theta)}{d\cos\theta} \right|^2 \\
&\quad + \frac{2}{3}\lambda^2 \left| \sum_l \frac{1}{\sqrt{2l(l+1)}} \left\{ l(l+1) \exp(i\delta_{l,l+1} + i\psi_l) \sin\delta_{l,l+1} \right. \right. \\
&\quad - l(l+1) \exp(i\delta_{l,l-1} + i\psi_l) \sin\delta_{l,l-1} \left. \left. \right\} \sin\theta \frac{dP_l(\cos\theta)}{d\cos\theta} \right|^2 \\
&\quad + \frac{2}{3}\lambda^2 \left| \sum_l \frac{1}{2l(l+1)} \left\{ l \exp(i\delta_{l,l+1} + i\psi_l) \sin\delta_{l,l+1} \right. \right. \\
&\quad - (2l+1) \exp(i\delta_{l,l} + i\psi_l) \sin\delta_{l,l} \\
&\quad \left. \left. + (l+1) \exp(i\delta_{l,l-1} + i\psi_l) \sin\delta_{l,l-1} \right\} \sin^2\theta \frac{d^2P_l(\cos\theta)}{(d\cos\theta)^2} \right|^2,
\end{aligned}$$

⁹ We are much indebted to Mr. Kurt Alder for producing this formula for us. The present form differs from that of J. M. Blatt and L. C. Biedenharn, *Revs. Modern Phys.* **24**, 258 (1952), in that the scattering matrix is assumed diagonal in l ; a discussion of this assumption follows in a later section.

where

$$A_e = -\frac{1}{2}\eta \csc^2(\theta/2) \exp(i\eta \ln \csc^2\theta/2); \quad \eta = e^2 Z_1 Z_2 / \hbar v;$$

$$\exp(i\psi_l) = \frac{(1+i\eta) \cdots (l+i\eta)}{(1-i\eta) \cdots (l-i\eta)}; \quad \psi_0 = 0;$$

$$\delta_{l,J} = \phi_l + \beta_{l,J}; \quad \tan\phi_l = -(F_l/G_l)_R;$$

$$\Gamma_\lambda = 2kR\gamma_\lambda / (F_l^2 + G_l^2)_R; \quad \tan\beta_{l,J} = \frac{1}{2}\Gamma_\lambda / (E_\lambda + \Delta_\lambda - E);$$

$$\Delta_\lambda = -\gamma_\lambda \left[\frac{d \ln(F_l^2 + G_l^2)^{1/2}}{d \ln kr} + l \right]_R.$$

The first two terms represent the part of the scattering in which the z component of the channel spin, m_s , is unchanged: these parts are individually coherent with the Coulomb scattering, represented by A_e . The third and fourth terms arise from the incoherent scattering with $\Delta m_s = \pm 1$, while the last comes from the case $\Delta m_s = \pm 2$. It is assumed that no change occurs in l , the orbital angular momentum. The adjustable parameters are the $\beta_{l,J}$, containing E_λ , Δ_λ , and Γ_λ , and R , the channel radius. As has been pointed out by Jackson and Galonsky,¹⁰ the E_λ and Γ_λ exert their main influence in the neighborhood of the resonance, while the choice of R is essentially determined by the off-resonance behavior of the cross section.

To a sufficiently good approximation for the present case, we may expand the quantity $\Delta(E)$ as a linear function of energy¹¹ and rewrite the argument of the resonant term as

$$\tan\beta_{l,J} = \frac{\frac{1}{2}\Gamma'}{E_{\text{res}} - E}$$

where

$$\Gamma' = \frac{\Gamma}{1 + \gamma b} \quad \text{and} \quad b = \left[\frac{d}{dE} \left(\frac{d \ln(F^2 + G^2)^{1/2}}{d \ln kr} \right) \right]_{R, E_{\text{res}}}$$

For a preliminary determination of the resonance parameters, one may use the observations at the two

TABLE III. Comparison of calculated and observed maximum cross sections for various assumed values of l and J . The calculations are based on a radius $R = 4.02 \times 10^{-13}$ cm and include contributions from only one resonance, with no change in l , plus non-resonant scattering for all waves.

l	J, π	$d\sigma/d\Omega_{\text{max}}$ (barns/sterad)	
		$\theta_{\text{cm}} = 156^\circ$	$\theta_{\text{cm}} = 120^\circ$
0	1+	0.26	0.24
1	0-	0.07	0.12
1	1-	0.17	0.17
1	2-	0.28	0.22
2	1+	0.72	0.42
2	2+	0.92	0.25
2	3+	1.39	0.38
Observed values:		1.49	0.40

¹⁰ H. L. Jackson and A. I. Galonsky, *Phys. Rev.* **89**, 370 (1952).

¹¹ R. G. Thomas, *Phys. Rev.* **81**, 148 (1951).

back angles since here the cross-section curves are fairly symmetrical and show no pronounced distortion from interference effects. Using the observed half-width, one can estimate $\Gamma'(E=E_{\text{res}})=23$ keV (c.m.s.). One finds, then, with a channel radius $R=4.02 \times 10^{-13}$ cm (i.e., $1.41 \times (2^{\frac{1}{2}}+4^{\frac{1}{2}}) \times 10^{-13}$ cm), values of $\gamma_2=1.25$ Mev and $\gamma_3=30$ Mev for the reduced widths corresponding to the assumptions of resonance formation by d and f waves, respectively. Since the Wigner limit for scattering of a single particle in a potential well is $\gamma_{SP} \sim \hbar^2/MR^2=2$ Mev, it would appear that $l > 2$ are excluded.¹²

Having, at least tentatively, narrowed the field to s , p , and d waves, we proceed to compare the absolute cross sections observed with those calculated from the scattering formula, assuming that only one level contributes to the resonance but taking into account the effects of Coulomb and potential scattering from all waves. These values are exhibited in Table III. It is evident that only $l=2$, $J=3^+$ gives a reasonable account of the observations although with rather generous stretching of the experimental errors and with due regard to the uncertainties in the assumptions underlying the calculation, $l=2$, $J=2^+$ might be regarded as a possibility. This choice is, however, ruled out by the observation at $\theta_{\text{cm}}=90^\circ$, where the calculation shows that the cross section should have a pronounced maximum for $J=2^+$ (shown by the dot-dashed curve of Fig. 9), whereas the curve for $J=3^+$ should have a minimum at this angle. The trend of the experimental points clearly excludes the former.

With the values of l and J thus established, one pro-

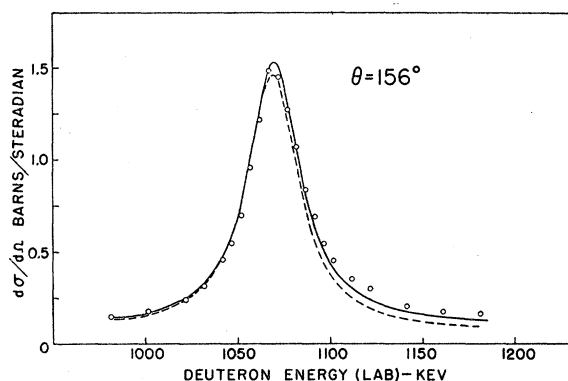


FIG. 7. Differential cross section at $\theta_{\text{cm}}=156^\circ$. The open circles are the same experimental points as those shown in Fig. 4. The dashed curve is calculated for one resonance, $J=3^+$, $l=2$, with a channel radius $R=5.0 \times 10^{-13}$ cm, whereas the solid curve is calculated for $R=4.02 \times 10^{-13}$ cm and includes the effect of the ground state.

¹² The application of single-particle models to so loosely-bound a structure as the deuteron in the calculation of the scattering formula and in the interpretation of the reduced width must be regarded as a dubious procedure. The solution of the three-body problem appears, however, to present a number of difficulties, and the fact that a reasonably good fit to the data is obtained with the present treatment may justify the use of this simple picture here. At higher energies, where dissociation of the deuteron is possible, a rather different formalism may be necessary.

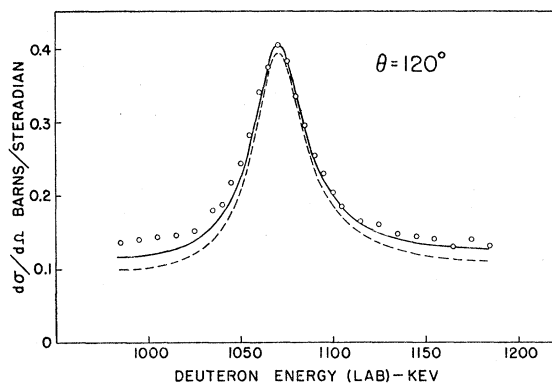


FIG. 8. Differential cross section at $\theta_{\text{cm}}=120^\circ$. Open circles are experimental points, repeated from Fig. 5. The dashed curve is calculated for one resonance, $J=3^+$, $l=2$, with $R=5.0 \times 10^{-13}$ cm, whereas the solid curve is calculated for $R=4.02 \times 10^{-13}$ cm and includes the effect of the ground state.

ceeds to attempt a more detailed fit to the cross-section data. The results of the first calculations, using $R=4.0 \times 10^{-13}$ cm and resonance parameters $E_{\text{res}}=1069$ keV, $\gamma=1.25$ Mev, are shown in the dot-dashed curves of Figs. 4, 5, and 6. It is evident that the agreement with the experimental points leaves much to be desired, particularly as regards the off-resonance cross section. The results of calculations with a somewhat larger channel radius, $R=6.55 \times 10^{-13}$ cm, in which the usual "radius" of the deuteron is used, are shown by the dashed curves of the same figures. Again, the fit to the experimental points is unsatisfactory. It may be observed that in the 156° data (Fig. 4) the larger radius actually moves the curve in the wrong direction at the high-energy end.

The best fit which can be obtained with the assumption of a single level is given by a radius of 5.0 to 5.4×10^{-13} cm. Calculated cross sections for a radius of 5.0×10^{-13} cm are shown in the dashed curves of Figs. 7, 8, and 9. At 90° (Fig. 9) the agreement with the experimental points is well within the estimated errors; at 120° (Fig. 8) the background both below and above resonance is low by 25 to 30 percent, or about twice the estimated error, and at 156° (Fig. 7) the background at the high end is low, again by about twice the estimated error. An increase of radius to 5.2×10^{-13} cm would improve the fit in the 120° case and would probably still be acceptable for the 90° data but would increase the discrepancy in the 156° curve.

Somewhat better agreement with the experimental data can be obtained by taking into account the effect of the ground state. The ground state of Li^6 has $J=1^+$ and can be formed by s -wave deuterons. Since it is evidently a fairly isolated state, it appears not unreasonable to assume that it has a large reduced width, and we have taken the width to be the same as for the $J=3^+$ state, $\gamma=1.25$ Mev. The characteristic energy, E_s , defined as the energy at which $f_0 \equiv (Ru_0'/u_0)_R=0$ is estimated with the help of a simple square-well model, utilizing the fact that there exists a bound state with

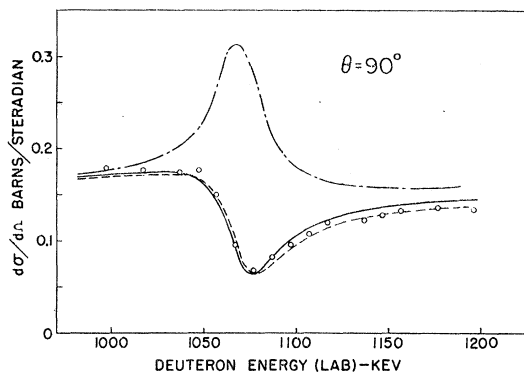


FIG. 9. Differential cross section at $\theta_{cm}=90^\circ$. The open circles are repeated from Fig. 6. The upper (dot-dashed) curve is for $J=2^+$, $l=2$, whereas the lower is calculated for $J=3^+$, $l=2$ with $R=5.0 \times 10^{-13}$ cm. The solid curve is calculated for $R=4.02 \times 10^{-13}$ cm and includes the effect of the ground state.

$J=1^+$ at 1.477 Mev (cm) below the deuteron-alpha separation energy. It is found that $E_s = -2.9 \frac{1}{2}$ Mev. With these parameters, and with the smaller channel radius, $R=4.0 \times 10^{-13}$ cm, one obtains the solid curves of Figs. 7, 8, and 9, which are seen to fit the experimental points well within the estimated uncertainties. The quality of the fit is, of course, rather sensitive to the choice of radius, and it is clear that the ground-state reduced width is only roughly determined by the present results. In fact, as has been shown above, the fit with the radius 5.0×10^{-13} cm, ignoring the ground state entirely, is not completely unacceptable, and it cannot be established with certainty that the effect of the ground state has been demonstrated in this experiment. It may be argued, however, that the assumption of a large reduced width for the ground state is not unreasonable and that the observations are entirely consistent with such an assumption.

The resonance energy $E_{lab} = 1069 \pm 2$ keV for the $J=3^+$ level agrees well with the value 1065 keV calculated from the Q value of Browne *et al.*,⁵ considering the uncertainty of nearly 40 keV introduced by the mass table. The width $\Gamma' = 23$ keV, corresponding to the value $\gamma = 1.25$ Mev used in calculating the cross-section curves, does not seem to be in so satisfactory agreement with the earlier reported value. However, we are

informed by Richards¹³ that the width quoted referred to the alpha-particle group width, and should be multiplied by $(\partial Q/\partial E_\alpha) = 2.08$ for the existing experimental conditions. This effect, together with some uncertainty as to the target thickness, allows an upper limit for the level width which is in good agreement with the present observations.

It was pointed out earlier that the scattering formula used here presupposes that the scattering matrix is diagonal in l . This assumption does not affect the non-resonant terms, and for the resonant terms the requirement of conservation of angular momentum and parity permits a change in l only for the cases $J=1^+$, 2^- , and 3^+ ($J \leq 3$). Here, l may change in the course of the scattering from $l=J+1$ to $J-1$ or conversely. The error introduced by ignoring these terms may be estimated by the use of Blatt and Biedenharn's formula⁹ assuming the same reduced width for both values of l . It is found that the correction amounts at most to 1.5 percent for $J=3^+$, 6 percent for $J=2^-$, and 10 percent for $J=1^+$ ($l=0$), for the two back angles, and accordingly has no significance for the present results.

We have also attempted in a preliminary way to account for the observations at 1.96 Mev of Blair *et al.*,⁴ using the parameters found in the present experiment. It appears that the present parameters lead to a much stronger dependence on angle at the back angles than is observed, and one is forced to the conclusion that at least one more state will be required to give an account of the higher-energy data.

We are deeply indebted to Professor N. Bohr for his interest in and encouragement of the present work. Mr. Kurt Alder, Mr. Aage Bohr, and Mr. Č. Zupančič have also contributed invaluable aid in both the experimental and theoretical aspects of the problem and we are grateful to Professor T. Gustafson and Dr. G. Källén for some fruitful discussions. One of us (S.G.N.) wishes to express his thanks to the Swedish Atomic Committee for financial support. Another of us (T.L.) is indebted to the U. S. Educational Foundation in Denmark and to the California Institute of Technology for financial support during his stay in Copenhagen.

¹³ H. T. Richards (private communication).